Available online at www.sciencedirect.com
ScienceDirect
Physica B 400 (2007) 297–306
PHYSICA B
www.elsevier.com/locate/physb

# First principles study of structural and electronic properties of different phases of boron nitride

Rashid Ahmed[a,*], Fazal-e-Aleem[a], S. Javad Hashemifar[b], Hadi Akbarzadeh[b]

[a]Centre for High Energy Physics, University of the Punjab, Lahore 54590, Pakistan
[b]Department of Physics, Isfahan University of Technology, 84156 Isfahan, Iran

Received 25 June 2007; received in revised form 27 July 2007; accepted 3 August 2007

**Abstract**

A theoretical study of structural and electronic properties of the four phases of BN (zincblende, wurtzite, hexagonal and rhombohedral) is presented. The calculations are done by full potential (linear) augmented plane wave plus local orbitals (APW + lo) method based on the density functional theory (DFT) as employed in WIEN2k code. Using the local density approximation (LDA) and generalized gradient approximation (GGA-PBE) for the exchange correlation energy functional, we have calculated lattice parameters, bulk modulus, its pressure derivative and cohesive energy. In order to calculate electronic band structure, another form of the generalized gradient approximation proposed by Engel and Vosko (GGA-EV) has been employed along with LDA and GGA-PBE. It is found that all the three approximations exhibit similar band structure qualitatively. However, GGA-EV gives energy band gap values closer to the measured data. Our results for structural and electronic properties are compared with the experimental and other theoretical results wherever these are available.


*Keywords:* Density functional theory; III–V Compounds; Boron nitride; Bandgap; WIEN2K; FPLAPW

## 1. Introduction

III–V semiconductors and their properties have been widely explored because of their use in electronic and optoelectronic devices. Boron nitride (BN) is one of the very interesting III–V binary compounds. Due to different modifications in structure, zincblende (cubic) boron nitride (c-BN), wurtzite boron nitride (w-BN), hexagonal boron nitride (h-BN) and rhombohedral boron nitride (r-BN), it exhibits some very fascinating physical properties such as extreme hardness, wide energy band gap, low dielectric constant, high thermal conductivity, chemical inertness and strong anisotropy. Owing to the wide spectrum of remarkable properties, its different phases have been the subject of theoretical and experimental studies for a long time [1–62]. It shares many of its structural properties with carbon as the cubic zincblende (c-BN) and wurtzite structures BN (w-BN) resemble cubic and hexagonal diamond structures [42,43,51]. Cubic BN has been reported most stable from ambient condition to very high pressure in recent measurements [61,63] but the final picture is still blurred. Wurtzite BN has been reported to be meta-stable at ambient conditions and thermodynamically stable at high pressure and high temperature [35].

Zincblende BN and w-BN are dense phases with $sp^3$-hybridized B–N bonds and a three-layer and a two-layer stacking sequences, respectively. Zincblende phase of BN depicts interesting physical properties such as extreme hardness, wide energy band gap, low dielectric constant and high thermal conductivity. It is acid resistant, stable against oxidation and very useful for cutting and shaping the iron- or nickel-containing materials used in industry [59]. It is also an excellent material for the protective coating of heavy-duty tools [3,4] and a good candidate as a pressure gauge at high temperature for diamond anvil cell experiments [55]. Hexagonal BN is a low-density phase with $sp^2$-hybridized B–N bonds and a two-layer stacking sequences with a wide band gap. It was a common belief that h-BN is a ground state of BN but some recent

*Corresponding author. Tel.: +92 42 9231137; fax: +92 42 9231253.
*E-mail address:* rasofi@hotmail.com (R. Ahmed).

0921-4526/$ - see front matter © 2007 Elsevier B.V. All rights reserved.
doi:10.1016/j.physb.2007.08.012

measurements have questioned this concept [61]. Hexagonal BN is extensively used in vacuum technology due to high thermal stability and is also employed in microelectronic devices [5], X-ray lithography masks [6] and as a wear resistant lubricants [7]. The hexagonal phase is also the fundamental structure of BN nanotubes, which are systems of growing interest [8–10,58]. Another low-density phase named as rhombohedral (r-BN) has also been reported with three-layer stacking sequence in literature. The r-BN is expected as a starting material for c-BN. In addition, some other layered phases of h-BN with $sp^2$ bonding have also been reported with different stacking sequence [52].

Development of new devices as well as operating characteristics of the devices based on certain materials depend on their properties and underlying science [63]. Although many studies have been performed to understand the physical properties of BN compounds, there are many aspects seeking clarity-like issue of the stability between h-BN and c-BN phases at ambient condition and electronic band gap controversy among different studies [12,20,39,42,51] for hexagonal phases. A comprehensive theoretical analysis of structural and electronic properties along with experimental results is therefore indispensable.

Computational methods using first principles have opened a new era in condensed matter physics. It is now possible to compute with accuracy the structural and electronic properties of solids, enabling us to explain and predict properties which are difficult to measure even experimentally [1]. From the end of last century, first-principles calculations based on density functional theory (DFT) [64,65] have become an essential part of research in material science. Most of these theoretical studies have been undertaken by using pseudo-potential [66] or FP-LAPW (one of the most accurate computational method for the study of crystalline solids) methods. These theoretical studies were performed using the DFT within the local density approximation (LDA) [67] or generalized gradient approximation (GGA-PBE) [68]. Although LDA and GGA give good results for ground state properties, it underestimates band gap energy values. Another form of GGA proposed by Engel and Vosko (GGA-EV) [69] successfully explains the electronic properties of different solids [70–79]. To the best of our knowledge, theoretical investigations of BN compound with GGA-EV have been rarely reported yet. In literature also, very little theoretical work has been reported about the study of electronic properties of different phases of BN with GGA-PBE. Therefore, a comprehensive study of different phases of BN based on full potential linearized augmented plane wave method provides very useful information.

The aim of this paper is to carry out a thorough DFT-based search to calculate structural and electronic properties for different phases of BN. These calculations have been performed by full potential (linear) augmented plane wave plus local orbitals ((L)APW + lo) method employing WIEN2k code [80,81]. Calculated lattice parameters, bulk moduli, its pressure derivative, cohesive energy and band structure were methodically analyzed. In addition, a systematic comparison of different forms of exchange correlation potentials is also presented. The paper is organized as follows: In Section 2, a brief description of our computational details is given. Results and discussion concerning the structural and electronic properties are presented in Section 3. A comparison with experimental and previous first principles computation is also provided. Finally, in Section 4 conclusions are drawn.

## 2. Computational details

Atomic electronic configuration of BN compound is B: He $2s^2 2p^1$ and N: He $2s^2 2p^3$. In our computation, we distinguish between the inner-shell electrons of B ($1s^2$) and N ($1s^2$) from the valence band electrons of B ($2s^2 2p^1$) and N ($2s^2 2p^3$). Atoms in zincblende BN structure are in fcc positions (space group $T_d^2 - F\bar{4}3m$) as B (0, 0, 0); N (1/4, 1/4, 1/4). Atoms in wurtzite structure of BN are in positions (space group $C_{6v}^4$(C6mc)) as B: (1/3, 2/3, 0), (2/3, 1/3, 1/2); N: (1/3, 2/3, $u$), (2/3, 1/3, 1/2 + $u$) where $u$ is taken as 0.375, in hexagonal structure of h-BN atoms are in positions $C_{6h}^3$(C6/mmc)as B: (1/3, 2/3, 1/4), (2/3, 1/3, 3/4); N: (2/3, 1/3, 1/4), (1/3, 2/3,3/4) and in rhombohedral modification of r-BN atoms are in positions as B: (0,0,0) and N: (2/3, 2/3, 2/3) with a space group $C_{3v}$ (R3m) in a primitive unit cell [82]. Our calculations were performed within the framework of DFT using the highly accurate all-electron full potential linear augmented plane wave plus local orbitals method as employed in WIEN2k code [80,81]. In this scheme, crystal unit cell is partitioned into two regions: non-overlapping Muffin-Tin (MT) spheres around each atom having their center at their atomic nuclei and the remaining interstitial area. In both regions of unit cell, Kohn–Sham wave functions, charge density and potential are expanded in the different sets of basis functions. For the wave functions, inside the MT spheres of radius ($R_{MT}$) around each atom, a linear combination of the atomic wave functions (radial solution of the Schrödinger equation) times the spherical harmonic expansion is used and in the interstitial region a plane wave expansion is used. The charge density and potential are expanded into lattice harmonics inside MT spheres and as a Fourier series in the remaining space. The maximum quantum number for atomic wave functions inside the MT sphere was $l_{max}$ equal to 10 and the energy cutoff for plane wave expansion of wave functions in the interstitial region was chosen to be $K_{max} = 8.0/R_{MT}$ while Fourier expanded charge density was truncated at $G_{max} = 14(\text{Ryd})^{1/2}$. To ensure total energy convergence, number of tests have been performed taking different $R_{MT}$ values and different sets of special $k$ points. In our calculations, $R_{MT}$ values for both B and N atoms are 1.4 a.u. in the zincblende and wurtzite structure. Whereas for h-BN and r-BN, $R_{MT}$ values for B and N are chosen as 1.3 and 1.37 a.u., respectively. Reciprocal space integration was performed by using an improved

tetrahedron method [83] and a mesh of 30 special $k$-points for zincblende, 114 for wurtzite, 72 for hexagonal and 84 for rhombohedral BN in the irreducible wedge of the Brillion zone. For the exchange correlation potential, Perdew and Wang formalism of the LDA and Perdew, Burke and Ernzerhof (PBE) formalism of the GGA have been applied. For band structure calculations, another form of generalized gradient approximation developed by Engel and Vosko (GGA-EV) is also used. Our calculations for the valence electrons were performed in a scalar-relativistic limit, while the core electrons were treated full relativistically. The spin orbit coupling was ignored as it does not affect the results considerably. More details of this scheme of calculations are available elsewhere [80,81].

## 3. Results and discussion

### 3.1. Structural parameters

A suitable choice of exchange correlation energy functional plays an important role for the accurate calculations of various properties of solids as in the total energy functional; 'exchange correlation' is approximated. In order to compute the structural properties of c-BN, w-BN, h-BN and r-BN, for the exchange correlation energy of electrons, LDA and GGA-PBE were employed within DFT. GGA-EV has not been used for calculating structural properties. It is adjusted for better reproduction of the exchange correlation potential at the expense of less accuracy in exchange correlation energy. This fact leads to less accurate values of total energy within this approximation and consequently obtained theoretical lattice parameters and other corresponding structural properties are far from the reality.

Total energy of primitive unit cell at different volumes is calculated over a range $\pm 10\%$ around equilibrium value for LDA and GGA-PBE exchange correlation potential for all phases of BN compound under study. To obtain equilibrium unit cell volumes, total energy of the crystal is minimized as a function of cell volume. By fitting the data thus obtained with Murnaghan equation of state [84], equilibrium lattice parameters, bulk modulus, its pressure derivative and cohesive energy were calculated which are listed in Table 1 along with available experimental data and other first principles works.

From Table 1, it is generally observed that LDA, compared with experiment, slightly underestimates the lattice parameters while GGA overestimates them. However, all computations for lattice parameters agree with the experimental numbers within 1% and 0.5% for LDA and GGA, respectively, except for rhombohedral phase. Table 1 shows that our results are in good agreement with other DFT-based calculations within LDA and GGA.

Bulk modulus, $B$, which is considered as a fundamental property to determine hardness of crystals, plays an important role in establishing stability criteria. The calculated values are shown in Table 1 together with available experimental and theoretical data. Bulk modulus of c-BN within LDA agrees well with experiment [24] with an error of about 0.7% along with previous first principles calculations for c-BN and w-BN whereas GGA underestimates the measured value by a factor of about 7%. Our calculated bulk modulus for c-BN and w-BN are close to each other and to that of diamond, 442 GPa as compared to other phases of BN. This may be due to the strong $sp^3$ B–N bonding and similar structure to diamond. The obtained bulk modulus for h-BN and r-BN are also close to each other but much lower than those of c-BN and w-BN because these non-cubic structures have a weak interaction along $c$-axis. Although our obtained bulk modulus for h-BN with LDA 254 and GGA 238 GPa are better than some others calculated values [20,25,42] but these are still substantially higher than experimental results. There is a wide spectrum of calculated results from 26.7 to 337 GPa that indicate a big theoretical discrepancy. This is attributed to the weakness of interactions along $c$-axis. The energy–volume data generated from isotropic compression and expansion of unit cells yield erroneous results for the bulk modulus, especially if the structures are strongly anisotropic [41,43]. The pressure derivatives of the bulk modulus have also been calculated (given in Table 1) and are in acceptable agreement with available measurements.

The cohesive energy, $E_{coh}$, defined as the difference between the total energy of isolated atoms and the total energy of crystal unit cell, was also calculated. The cohesive energy is another parameter that measures stability of materials. Despite many studies [6,7,11,20,33,38,43] it is not yet very clear as to which phase of BN is more stable at different temperatures and pressures. Comparison of cohesive energy in different phases may help to clarify this ambiguity. To obtain a precise value of this parameter, energy calculations for isolated atoms and crystal have been performed. In Table 1, we present computed cohesive energies of all BN phases by using LDA and GGA. A good agreement is observed with the other first principles data, given in the Table 1. It is known that LDA over-binds cohesive energy while GGA corrects this over-binding and hence is more reliable in this regard. This trend is also visible in our results and we found that LDA generally gives higher cohesive energies than GGA while the latter provides a good agreement with experiment. The cohesive energy calculated by using Hartree Fock (HF) [19] method is significantly lower than the experimental and DFT-based theoretical results. A negligible difference is observed between the cohesive energies of c-BN and w-BN phases. Similarly cohesive energies of h-BN and r-BN are also very close to each other. Our GGA results for c-BN (13.95 eV) and h-BN (14.11 eV) show that h-BN is more stable which is also evident from Fig. 1, drawn for energy–volume curves of c-BN, w-BN, h-BN and r-BN. Similarly our results with LDA also show that h-BN is more stable. There is no experimental result for comparison which warrants further experimental study in this direction.

Table 1
The calculated equilibrium lattice constant ($a$), volume ($V$), bulk modulus ($B$), its pressure derivative ($B'$) and cohesive energy ($E_{coh}$) using FP-L(APW + lo) calculations within LDA and GGA-PBE of zincblende, wurtzite, hexagonal and rhombohedral phases of BN compound compared with other first principles and experimental results

| Compounds | Method | Lattice parameters | | $V$ (a.u.)$^3$ | $B$ (GPa) | $B'$ | $E_{coh}$ (eV) |
|---|---|---|---|---|---|---|---|
| | | $a$ (Å) | $c$ (Å) | | | | |
| BN (zincblende) | | | | | | | |
| Our work | FP-LDA | 3.585 | – | 77.7 | 404 | 3.86 | 15.96 |
| | FP-GGA | 3.629 | – | 80.6 | 371 | 3.83 | 13.95 |
| Experiment | – | 3.615 [3] | – | – | 400 [24] | 3.00 [24] | 13.20 [6] |
| | | – | – | – | 387 [62] | 4±0.2 [6] | 13.60 [7] |
| Other calculation | PP-LDA | 3.606 [11] | – | – | 367 [11] | – | 14.3 [11] |
| | OLCAO-LDA | – | – | – | 370 [20] | – | 14.0 [20] |
| | LMTO-LDA | 3.62 [26] | – | – | 378 [26] | 3.80 [20] | |
| | FP-LMTO-LDA | 3.590 [31] | – | – | 400 [31] | 3.4 [26] | – |
| | PP-LDA | 3.593 [33] | – | – | 395 [33] | 4.10 [31] | 12.94 [33] |
| | PP-LDA | 3.576[25] | – | – | 397 [25] | 3.65 [33] | 16.30 [25] |
| | PP-VASP | 3.581 [38] | – | – | 398 [38] | 3.59 [25] | 16.31 [38] |
| | FP-LDA | 3.606 [9] | – | – | 367 [9] | – | – |
| | PP-LDA | 3.623 [46] | – | – | 368 [46] | – | – |
| | PP-LDA | 3.574 [42] | – | – | 401 [42] | 3.38 [46] | – |
| | PP-LDA | 3.592 [41] | – | – | 395 [41] | – | 16.00 [41] |
| | FP-LAPW-LDA | 3.630 [44] | – | – | 386 [44] | – | 17.39 [44] |
| | FP-LAPW-LDA | 3.583 [43] | – | – | 396 [43] | – | 16.31 [43] |
| | FP-LAPW-GGA | 3.633 [43] | – | – | 401 [43] | 3.96 [43] | 13.86 [43] |
| | PP-LDA | 3.582 [48] | – | – | 392 [48] | 3.00 [43] | – |
| | FP-LAPW-GGA | 3.623 [54] | – | – | 368 [54] | 3.76 [48] | – |
| | PP-GGA | 3.58 [60] | – | – | 380 [60] | 3.56 [60] | – |
| | HF | – | – | – | – | – | 09.10 [19] |
| BN(wurtzite) | | | | | | | |
| Our work | FP-LDA | 2.525 | 4.182 | 155.88 | 403 | 3.78 | 14.77 |
| | FP-GGA | 2.556 | 4.234 | 161.7 | 371 | 3.8 | 13.93 |
| Experiment | – | 2.553 [6] | 4.228 [6] | – | – | – | – |
| Other calculations | OLCAO-LDA | 2.536 [21] | 4.199 [21] | – | 390 [20] | 6.30 [20] | – |
| | FP-LMTO-LDA | 2.540 [31] | 4.170 [31] | – | 397 [31] | 3.70 [31] | – |
| | PP-LDA | 2.521 [25] | – | – | 401 [25] | 3.59 [25] | 16.04 [25] |
| | LMTO-LDA | – | – | – | 391 [26] | 3.7 [26] | – |
| | PP-LDA | 2.532 [33] | – | – | 394 [33] | 3.69 [33] | 12.96 [33] |
| | PP-LDA | 2.532 [41] | 4.188 [41] | – | 396 [41] | – | 15.97 [41] |
| | FP-LAPW-LDA | 2.525 [43] | 4.192 [43] | – | 408 [43] | 3.22 [43] | 16.27 [43] |
| | FP-LAPW-GGA | 2.557 [43] | 4.250 [43 | – | 366 [43] | 3.74 [43] | 13.80 [43] |
| BN (hexagonal) | | | | | | | |
| Present work | FP-LDA | 2.491 | 6.613 | 240.37 | 254 | 3.86 | 16.65 |
| | FP-GGA | 2.519 | 6.699 | 248.44 | 238 | 3.98 | 14.11 |
| Experiment | – | 2.504 [30] | 6.660 [30] | – | 36.7[29] | – | – |
| Other calculation | OLCAO-LDA | – | – | – | 335 [20] | 2.48 [20] | – |
| | FP-LDA | 2.468 [25] | 6.392 [25] | – | 261 [25] | 3.66 [25] | – |
| | PP-VASP | 2.489 [38] | 6.481 [38] | – | 28 [38] | – | 16.19 [38] |
| | PP-LDA | 2.486 [42] | 6.484 [42] | – | 268 [42] | – | – |
| | PP-LDA | 2.496 [41] | 6.498 [41] | – | 26 [41] | – | 15.89 [41] |
| | FP-LAPW-LDA | 2.495 [43] | 6.437 [43] | – | 26.7[43] | 10.7 [43] | 16.16 [43] |
| | FP-LAPW-GGA | 2.517 [43] | 8.397 [43] | – | 2.13[43] | 9.6 [43] | 14.01 [43] |
| | DFT-LDA | 4.485 [51] | 6.490 [51] | – | – | – | – |
| BN (rhombohedral) | | | | | | | |
| Present work | FP-LDA | 2.254 | 8.109 | 120.35 | 253 | 3.78 | 16 |
| | FP-GGA | 2.276 | 8.19 | 124 | 228 | 4.67 | 14.15 |
| Experiment | – | – | – | – | – | – | – |
| Other calculation | PP-VASP | 2.48 [50] | 9.65 [50] | – | – | – | – |
| | PP-LDA | 2.493[33] | 3.231[33] | – | 32.2[33] | 10.3[33] | 13.05[33] |

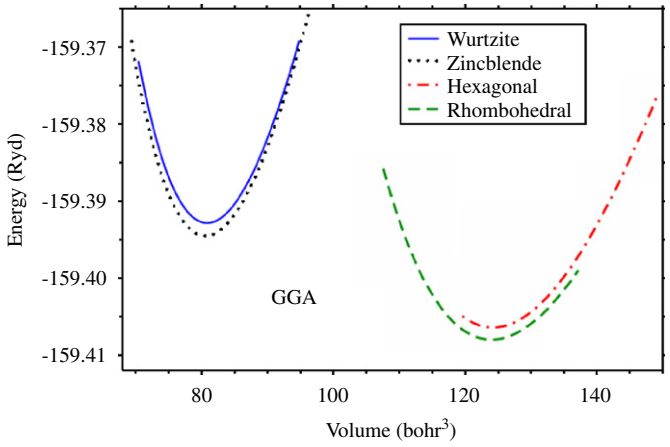


Fig. 1. Energy–volume curves for c-BN, w-BN, h-BN and r-BN with GGA-PBE.

### 3.2. Electronic band structure calculations

Although our calculated values of lattice parameter using LDA and GGA are close to the experiment, due to high sensitivity of electronic band gap to lattice parameters, we have used experimental values of lattice parameters for consistent study of electronic structure using different exchange correlation approximations. By using experimental lattice parameters, eigenvalues of Kohn–Sham equations were calculated with (FP-L(APW + lo)) method along some high symmetry directions in the Brillion zone. For the exchange correlation potential, LDA, GGA-PBE and GGA-EV have been used. The obtained band structures are presented in Figs. 2–13 and corresponding calculated band gaps, $E_g$, are given in Table 2 along with other first principles and experimental data whenever these are available.

For all phases, we observe that the three different exchange correlation approximations lead to the similar band structures and the main difference is in the numerical value of the energy band gap. As it is mentioned in Table 2, all BN phases have a theoretically indirect band gap that agrees well with available experiments. In the case of c-BN all other theoretical works also predict the true experimental direction of the band gap while for w-BN and h-BN the predicted direction of the band gap in some theoretical studies contradicts with experiment. Even in the case of h-BN only our results could confirm the K–M direction of the band gap observed in experiment and we did not find any other successful theoretical study in this regard. In the r-BN phase, the maxima of the valence band lies between H and N points while the minima of the conduction band lies at N point. To our knowledge there are no first principles and experimental reports available for electronic properties for r-BN. Our work is thus a first attempt in this direction.

The calculated band gap values are almost the same within LDA and GGA-PBE while GGA-EV apparently enhances them to become closer to the measured data (Table 2). The observed similarity between LDA and GGA

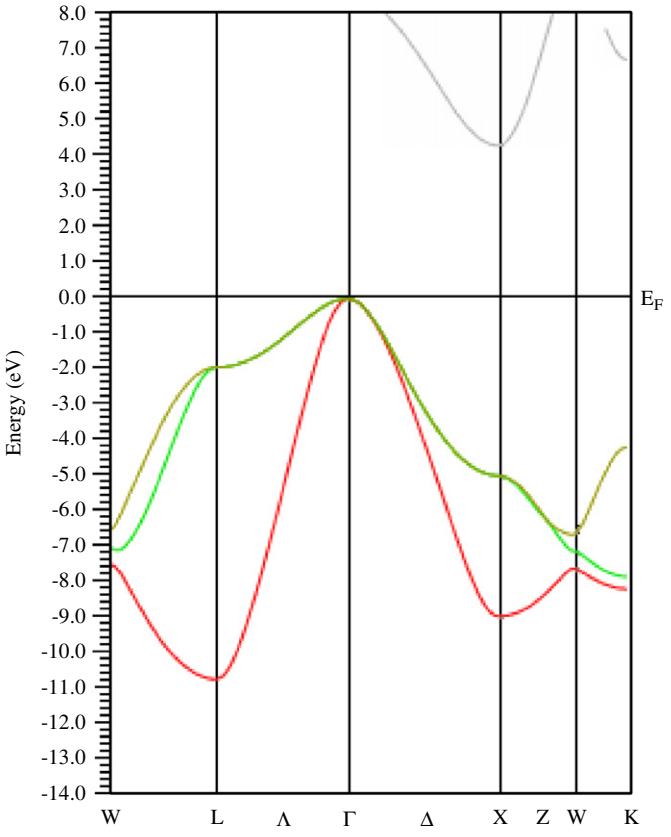


Fig. 2. Band structure of c-BN using LDA.

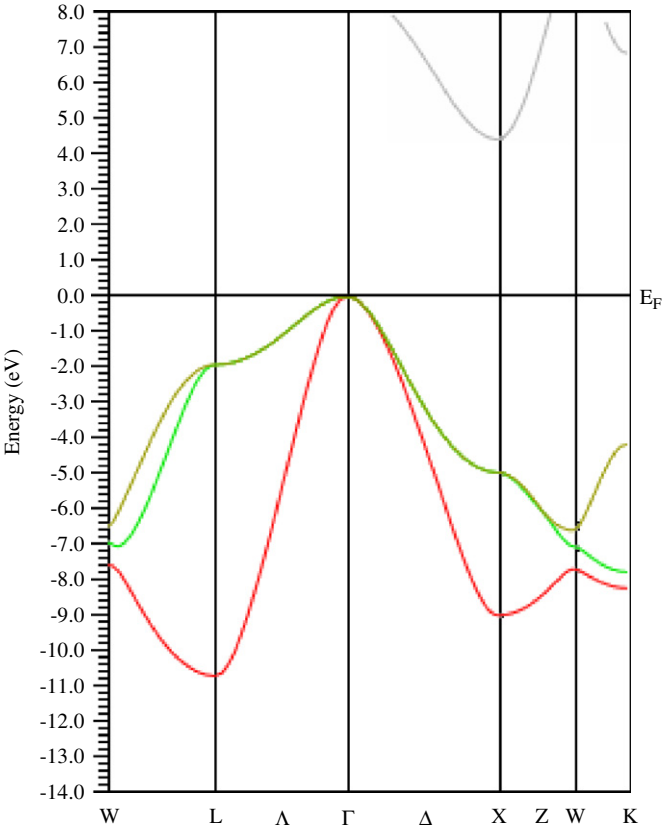


Fig. 3. Band structure of c-BN using GGA-PBE.

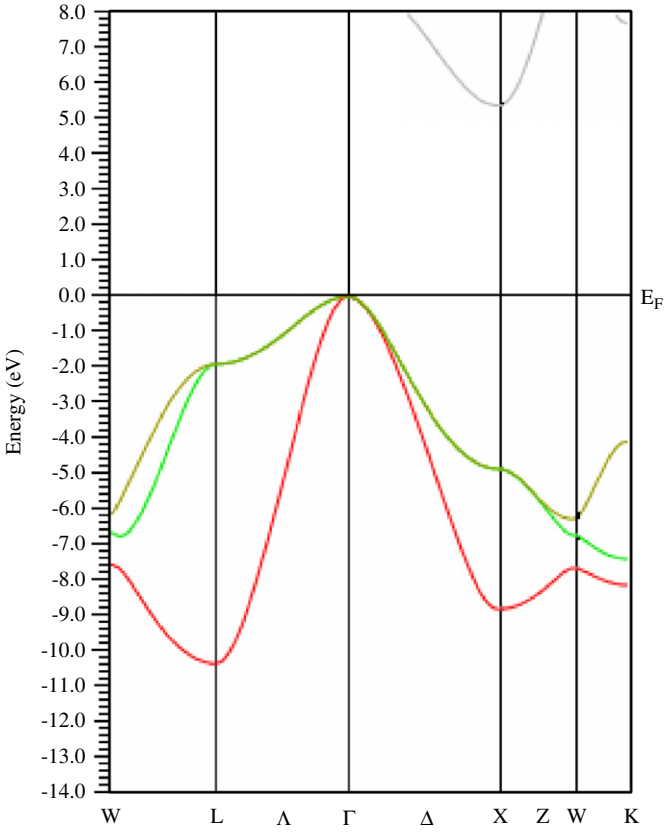


Fig. 4. Band structure of c-BN using GGA-EV.

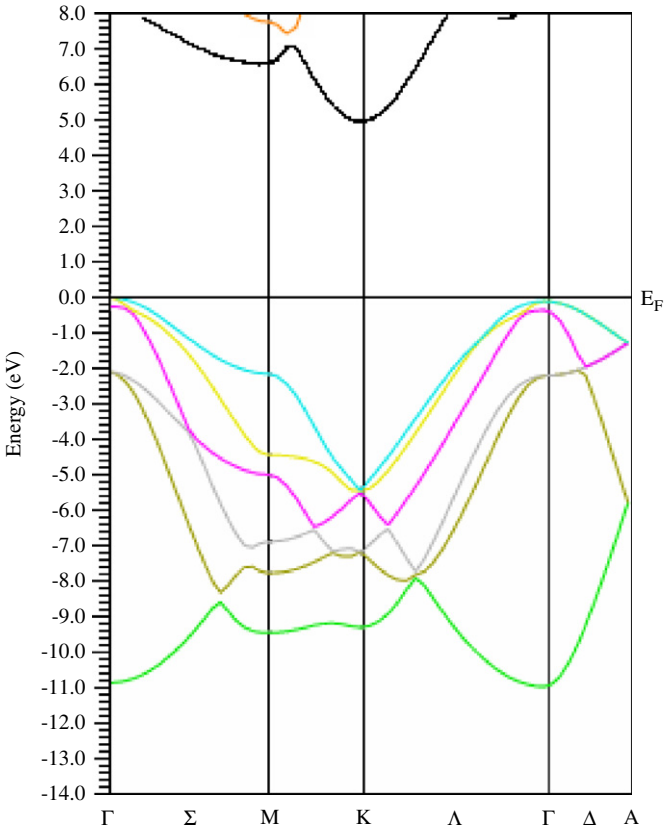


Fig. 5. Band structure of w-BN using LDA.

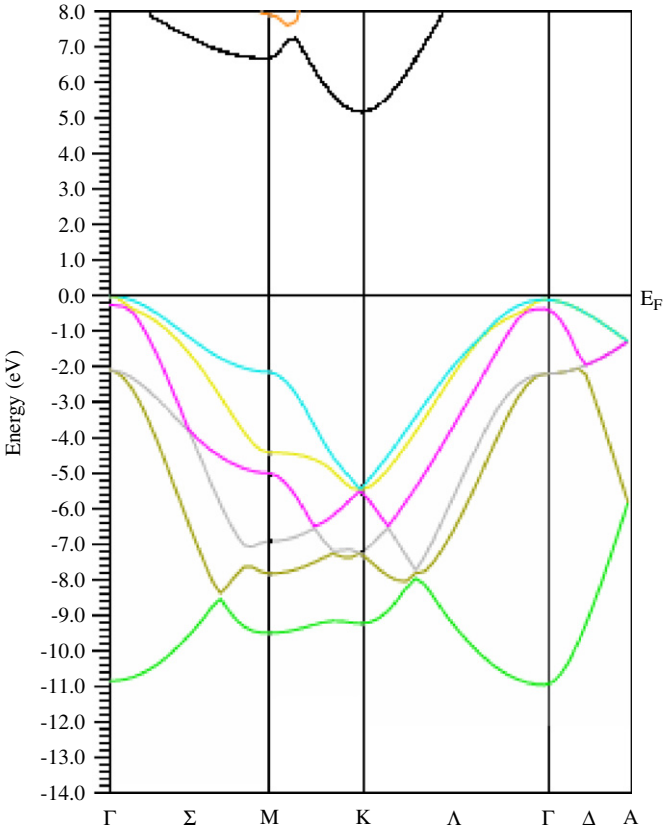


Fig. 6. Band structure of w-BN using GGA-PBE.

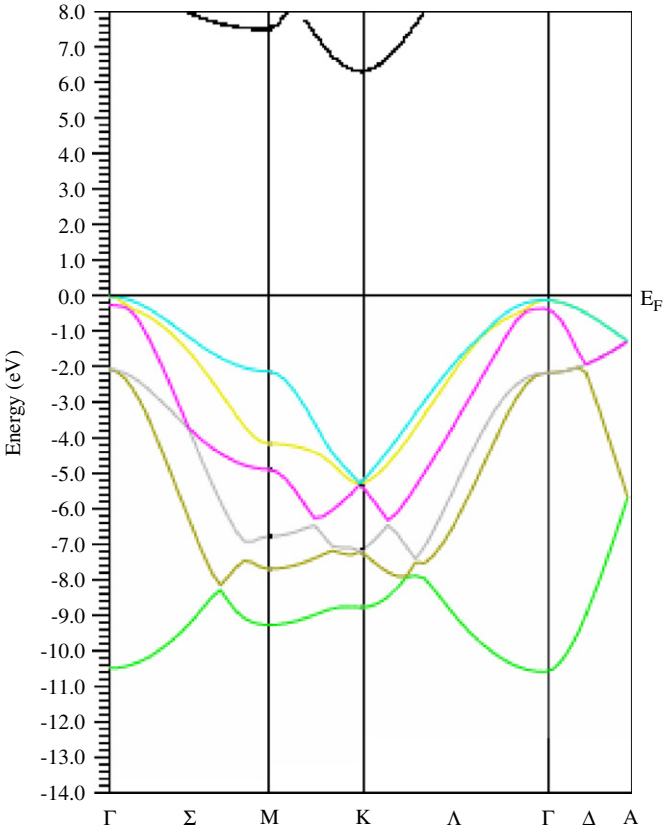


Fig. 7. Band structure of w-BN using GGA-EV.

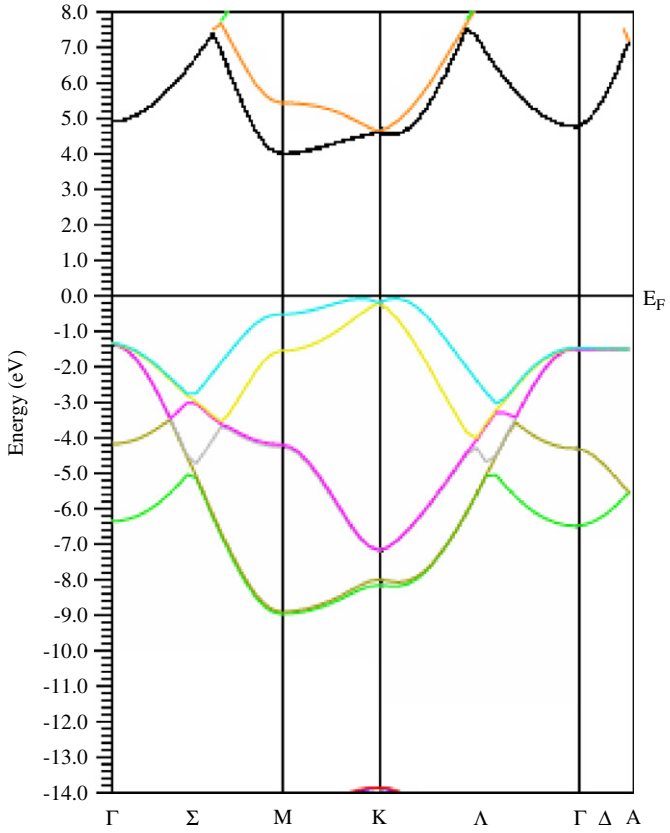


Fig. 8. Band structure of h-BN using LDA.

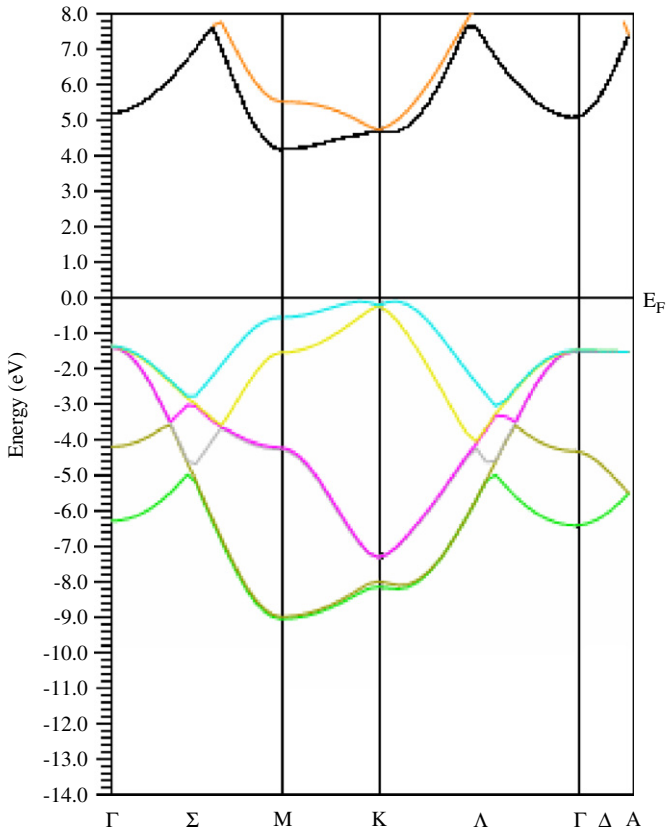


Fig. 9. Band structure of h-BN using GGA-PBE.

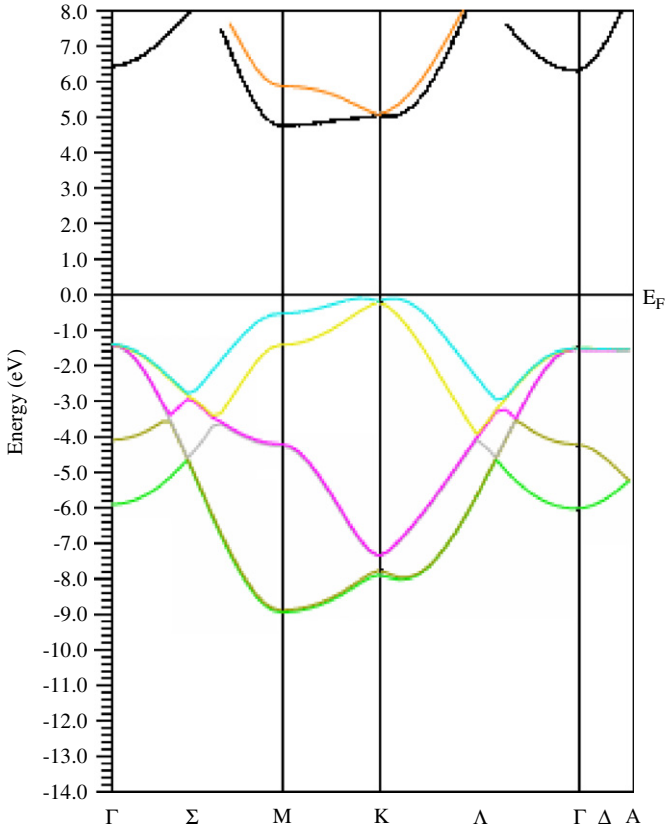


Fig. 10. Band structure of h-BN using GGA-EV.

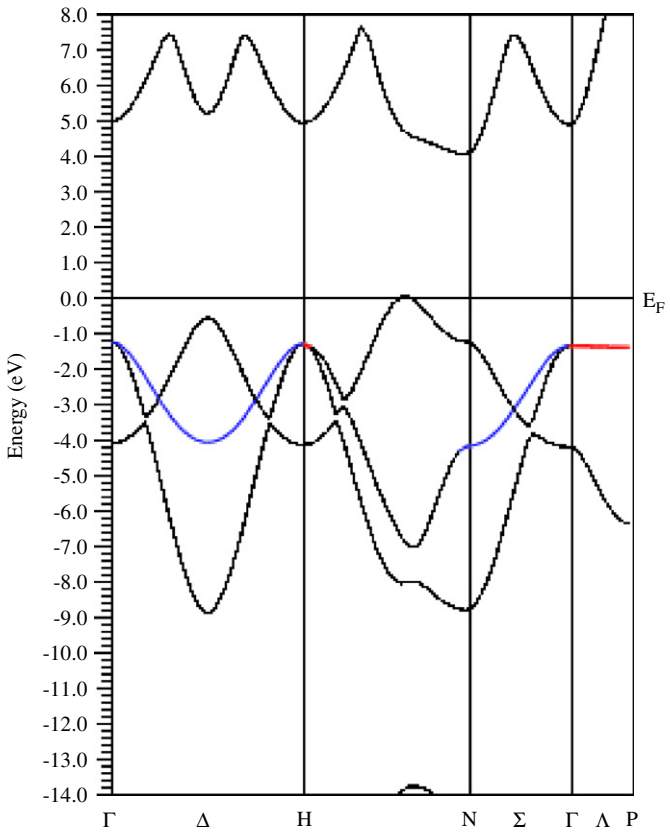


Fig. 11. Band structure of r-BN using LDA.

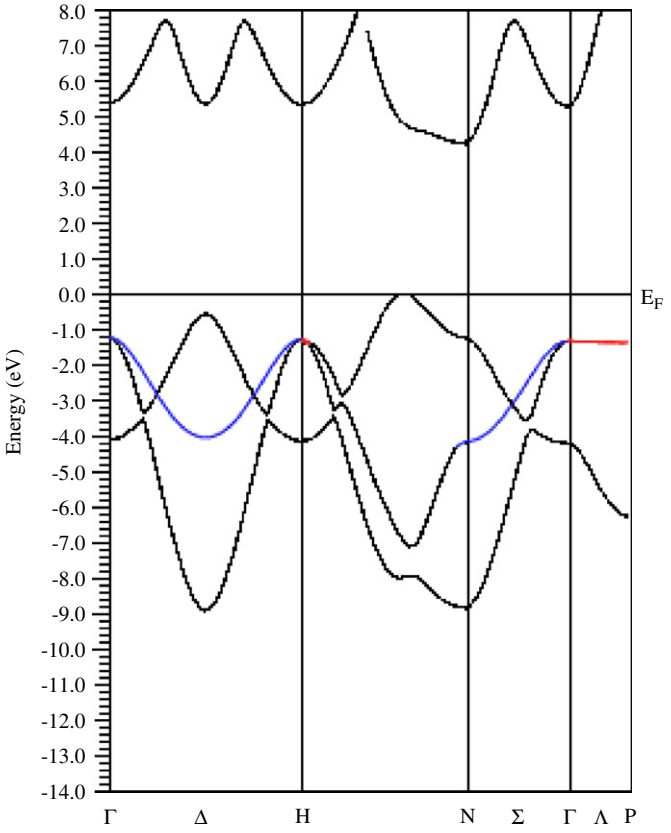


Fig. 12. Band structure of r-BN using GGA-PBE.

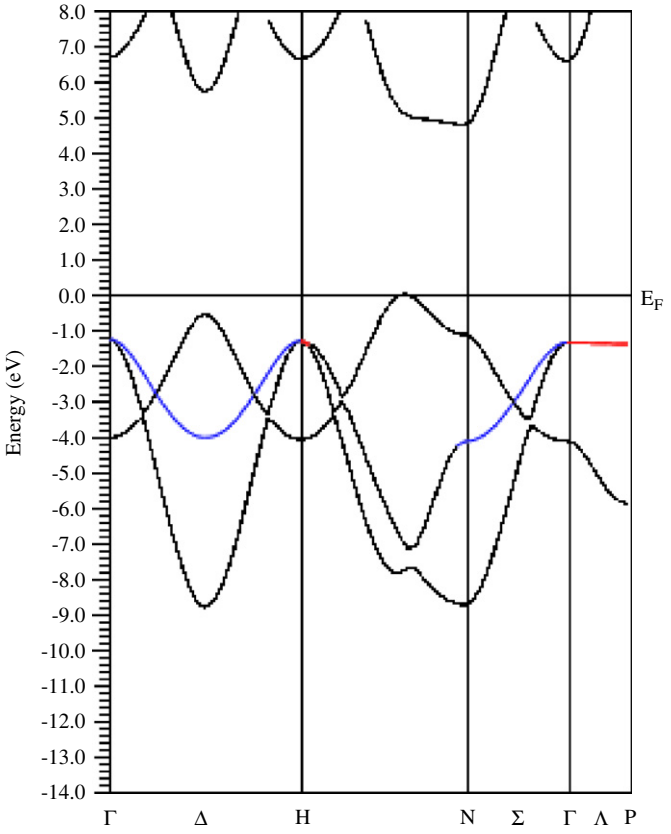


Fig. 13. Band structure of r-BN using GGA-EV.

Table 2
Energy band gap ($E_g$) properties for different phases of BN compound compared with other first principles and experimental results whereever are available

| Compound | Methods | XC | $E_g$(eV) | Type of band gap |
|---|---|---|---|---|
| BN(zincblende) | | | | |
| Present work | FP-LAPW | LDA | 4.35 | Indirect (Γ−X) |
| | | GGA | 4.47 | Indirect (Γ−X) |
| | | GGA-EV | 5.43 | Indirect (Γ−X) |
| Experiment | – | – | 6.0 [5] | Indirect (Γ−X) |
| | – | – | 6.1 [39] | Indirect (Γ−X) |
| Other Calculations | PP-PW | LDA | 4.2 [9,10,11] | Indirect (Γ−X) |
| | OLCAO | LDA | 5.18 [20] | Indirect (Γ−X) |
| | LMTO | LDA | 4.42 [26] | Indirect (Γ−X) |
| | FP-LMTO | LDA | 4.40 [31] | Indirect (Γ−X) |
| | FP-LAPW | GGA | 4.45 [46] | Indirect (Γ−X) |
| | PP-PW | LDA | 7.28 [42] | Indirect (Γ−X) |
| | FP-LAPW | LDA | 4.45 [44] | Indirect (Γ−X) |
| | PP-PW | LDA | 8.392[48] | Indirect (Γ−X) |
| | FPLO | LDA | 5.74 [53] | Indirect (Γ−X) |
| BN(wurtzite) | | | | |
| Present work | FP-LAPW | LDA | 5.0 | Indirect (Γ−K) |
| | | GGA | 5.23 | Indirect (Γ−K) |
| | | GGA-EV | 6.39 | Indirect (Γ−K) |
| Experiment | – | – | – | Indirect (Γ−K) |
| Other calculations | OLCAO | LDA | 5.81 [20] | Indirect (Γ−X) |
| | OLCAO | LDA | 5.81 [21] | Indirect (Γ−X) |
| | LMTO | LDA | 5.45 [26] | Indirect (Γ−K) |
| | FPLO | LDA | 7.70 [53] | Indirect (Γ−K) |
| BN(hexagonal) | | | | |
| Present work | FP-LAPW | LDA | 4.04 | Indirect (K−M) |
| | | GGA | 4.25 | Indirect (K−M) |
| | | GGA-EV | 4.83 | Indirect (K−M) |
| Experiment | – | – | 5.4 [39] | Indirect (K−M) |
| Other calculations | FP-LAPW | LDA | 3.9 [12] | Indirect (H−M) |
| | OLCAO | LDA | 4.07 [20] | Indirect (H−M) |
| | PP-PW | LDA | 6.39 [42] | Indirect (H−M) |
| | DFT | LDA | 4.027[51] | Indirect (H–M) |
| BN(rhombohedral) | | | | |
| Present work | FP-LAPW | LDA | 4.02 | Indirect (HN−N) |
| | | GGA | 4.23 | Indirect (HN−N) |
| | | GGA-EV | 4.79 | Indirect (HN−N) |
| Experiment | – | – | – | – |
| Other calculations | – | – | – | – |

XC, exchange correlation approximation.

band gaps are attributed to the lightness of B and N atoms. Since variation of the electronic charge density in the light elements is small, hence the charge density gradient corrections involved in GGA are not large and consequently this exchange correlation functional gives similar results to LDA that is based on a uniform electron gas approximation with no gradient correction. The observed enhancement of energy band gap within GGA-EV roots in the special theoretical basis used for developing this exchange correlation functional. It is well known that GGA-PBE underestimates the energy band gap of semiconductors that is due to its functional form which is not flexible enough to simultaneously reproduce accurately both exchange correlation energy and its charge derivative. GGA-EV has been developed in such a way that it optimizes the exchange correlation potential at the cost of less accuracy in exchange correlation energy. In this way it yields better band splitting and properties, which mostly depend on exchange correlation potential. Accordingly our calculated energy band gaps within GGA-EV are in better agreement with available experimental values. For w-BN and r-BN phases no experimental data are available but following the general trend of other III nitrides [75], it may be predicted that the band gap of w-BN should be close to the zincblende phase. Therefore, reasonably and hopefully, the calculated band gap of w-BN within GGA-EV would be close to reality.

## 4. Conclusion

We used DFT-FP-LAPW calculations to study the structural and electronic properties of zincblende (c-BN), wurtzite (w-BN), hexagonal (h-BN) and rhombohedral (r-BN) phases of BN compound. No comprehensive theoretical work is available on the study of different phases of BN, especially on r-BN. The calculated cohesive energy values within LDA and GGA-PBE indicate that h-BN is more stable than c-BN. For the first time, we used GGA-EV exchange correlation approximation to calculate the energy band structure of the BN structures. The results show that, thanks to the better treatment of the exchange correlation potential, GGA-EV enhance the energy band gaps compared with LDA and GGA-PBE and make them closer to the experimental data.

## Acknowledgments

Part of work was done at ICTP affiliated Center, Isfahan University of Technology, Iran. One of the authors (R.A.) acknowledges the financial support of the Isfahan University of Technology and University of the Punjab Lahore, Pakistan.

## References

[1] R. Khenata, H. Baltache, M. Sahnoun, M. Driz, M. Rerat, B. Abbar, Physica B 336 (2003) 321;
H. Arabi, A. Pourghazi, F. Ahmadian, Z. Nourbakhsh, Physica B 373 (2006) 16.
[2] A. Mujica, A. Rubio, A. Munoz, R.J. Needs, Rev. Mod. Phys. 75 (3) (2003) 863;
I. Vurgaftman, J.R. Meyer, L.R. Ram-Mohan, J. Appl. Phys. 89 (2001) 5815.
[3] R.H. Wentorf Jr., J. Chem. Phys. 26 (1957) 956.
[4] H.R. Philipp, E.A. Taft, Phys. Rev. 127 (1962) 159;
J.H. Edgar, Properties of group III nitrides, in: J.H. Edgar (Ed.), Institution of Electric Engineers, Stevenage, UK, 1994, pp. 7–21.
[5] V.A. Fomichev, M.A. Rumsh, J. Chem. Phys. 48 (1968) 555.
[6] T. Soma, S. Sawaoka, S. Saito, Mater. Res. Bull. 9 (1974) 755;
P.K. Lam, R.M. Wentzcovitch, M.L. Cohen, Synthesis and properties of boron nitride, in: J.J. Pouch, S.A. Alterovitz (Eds.), Materials Science Forum, vols. 54, 55, Trans Tech Publications, Zurich, Switzerland, 1990, p. 165.
[7] Numerical data and functional relationship in science and technology, in: O. Madelung (Ed.), Landolt Bornstein, New Series, vol. 17a, Springer, Berlin, 1982.
[8] A. Catellani, M. Posternak, A. Balderschi, H.J.F. Jansen, A.J. Freeman, Phys. Rev. B 32 (1985) 104102-1.
[9] R.M. Wentzcovitch, M.L. Cohen, J. Phys. C 19 (1986) 6791.
[10] R.M. Wentzcovitch, K.J. Chang, M.L. Cohen, Phys. Rev. B 34 (1986) 1071.
[11] R.M. Wentzovitch, M.L. Cohen, Phys. Rev. B 36 (1987) 6058.
[12] A. Catellani, M. Posternak, A. Balderschi, A.J. Freeman, Phys. Rev. B 36 (1987) 6105.
[13] K. Miyoshi, D.H. Bukley, J.J. Pouch, S.A. Alterovitz, H.E. Sliney, Surf. Coat. Technol. 33 (1987) 221.
[14] R.M. Wentzcovitch, S. Fahy, M.L. Cohen, S.G. Louie, Phys. Rev. B 38 (1988) 6191.
[15] E. Knittle, R.M. Wentzcovitch, R. Jeanloz, M.L. Cohen, Nature 337 (1989) 349.
[16] T.K. Pauli, P. Bhattacharya, D.N. Bose, Appl. Phys. Lett. 56 (1990) 2648.
[17] S.S. Dana, Mater. Sci. Forum 54–55 (1990) 229.
[18] E.K. Takahashi, A.T. Lino, A.C. Ferraz, J.R. Leite, Phys. Rev. B 41 (1990) 1691.
[19] R. Causa, R. Dovesi, C. Roetti, Phys. Rev. B 43 (1991) 11937.
[20] Y.-N. Xu, W.Y. Ching, Phys. Rev. B 44 (1991) 7787.
[21] Y.-N. Xu, W.Y. Ching, Phys. Rev. B 48 (1993) 4335.
[22] X. Blase, A. Rubio, S.G. Louie, M.L. Cohen, Europhys. Lett. B 28 (1994) 335.
[23] A. Rubio, J.L. Corkill, M.L. Cohen, Phys. Rev. B 49 (1994) 5081.
[24] M. Grimsditch, E.S. Zouboulis, A. Polian, J. Appl. Phys. 76 (1994) 832.
[25] J. Furthmüller, J. Hafner, G. Kresse, Phys. Rev. B 50 (1994) 15606.
[26] N.E. Christensen, I. Gorczyca, Phys. Rev. B 50 (1994) 4397.
[27] D.L. Medin, T.A. Friedmann, P.B. Mirkarimi, M.J. Mills, K.F. McCarty, Phys. Rev. B 50 (1994) 7884.
[28] X. Blase, A. Rubio, S.G. Louie, M.L. Cohen, Phys. Rev. B 51 (1995) 6868.
[29] V.L. Solozhenko, G. Will, F. Elf, Solid State Commun. 96 (1995) 1.
[30] S. Bohr, R. Haubner, B. Lux, Diamond Relat. Mater. 4 (1995) 714.
[31] K. Kim, W.R.L. Lambrecht, B. Segall, Phys. Rev. B 53 (1996) 16310.
[32] P.H. Philipsen, E.J. Baerends, Phys. Rev. B 54 (1996) 5326.
[33] K. Albe, Phys. Rev. B 55 (1997) 6203.
[34] J.C. Boettger, Phys. Rev. B 55 (1997) 11202.
[35] K. Karch, F. Bechstedt, Phys. Rev. B 56 (1997) 7404.
[36] W. Sekkal, B. Bouhafs, H. Aourag, M. Cartier, J. Phys: Condens. Matter 10 (1998) 4975.
[37] M. Ferhat, B. Bouhafs, A. Zaoui, H. Aourag, J. Phys: Condens. Matter 10 (1998) 7995.
[38] G. Kern, G. Kresse, J. Hafner, Phys. Rev. B 59 (1999) 8551.
[39] K.L. Jablonska, T. Suski, I. Gorczyca, N.E. Christensen, K.E. Attenkofer, R.C.C. Perera, E.M. Gullikson, J.H. Underwood, D.L. Ederer, Z. Liliental Weber, Phys. Rev. B 61 (2000) 16623.
[40] L. Bourgeois, Y. Bando, T. Sato, J. Phys. D 33 (2000) 1902.

[41] N. Ohba, K. Miwa, N. Nagasako, A. Fukumoto, Phys. Rev. B 63 (2001) 115207.
[42] G. Cappellini, G. Satta, M. Palummo, G. Onida, Phys. Rev. B 64 (2001) 035104.
[43] A. Janotti, S.-H. Wei, D.J. Singh, Phys. Rev. B 64 (2001) 174107.
[44] L.E. Ramos, L.K. Teles, L.M.R. Scolfaro, J.L.P. Castineira, A.L. Rosa, J.R. Leite, Phys. Rev. B 63 (2001) 115210.
[45] P.P. Rushton, S.J. Clark, D.J. Tozer, Phys. Rev. 63 (2001) 115206.
[46] A. Zaoui, F. El Haj Hassan, J. Phys.: Condens. Matter 13 (2001) 253.
[47] M. Fuchs, J.L.F. Da Silva, C. Stampfl, J. Neugebauer, M. Scheffler, Phys. Rev. 65 (2002) 245212.
[48] S.Q. Wang, H.Q. Ye, Phys. Rev. B 66 (2002) 235111.
[49] M. Castreich, J.D. Gale, C.M. Marian, Phys. Rev. B 68 (2003) 094110.
[50] W.J. Yu, W.M. Lau, S.P. Chan, Z.F. Liu, Q.Q. Zheng, Phys. Rev. B 67 (2003) 014108.
[51] L. Liu, Y.P. Feng, Z.X. Shen, Phys. Rev. B 68 (2003) 104102.
[52] T. Oku, K. Hiraga, T. Matsuda, T. Hirai, M. Hirabayashi, Diamond Relat. Mater. 12 (2003) 1138 & references therein.
[53] Y. Al-Douri, Solid State Commun. 132 (2004) 465.
[54] F. El Haj Hassan, H. Akbarzadeh, M. Zoaeter, J. Phys.: Condens. Matter 16 (2004) 293.
[55] F. Datchi, B. Canny, Phys. Rev. B 69 (2004) 144106.
[56] S. Guerini, P. Piquini, Phys. Rev. B 71 (2005) 193305.
[57] H. Lorenz, I. Orgzall, Scr. Mater. 52 (2005) 537.
[58] G.Y. Guo, J.C. Lin, Phys. Rev. B 71 (2005) 165402.
[59] J.B. MacNaughton, A. Moewes, R.G. Wilks, X.T. Zhou, T.K. Sham, T. Taniguchi, K. Watanabe, C.Y. Chan, W.J. Zhang, I. Bello, S.T. Lee, H. Hofsäss, Phys. Rev. B 72 (2005) 195113.
[60] H.M. Tütüncü, S. Bagci, G.P. Srivastava, A.T. Albudak, G. Ugur, Phys. Rev. B 71 (2005) 195309.
[61] N. Ooi, V. Rajan, J. Gottlieb, Y. Catherine, J. B Adams, Modell. Simul. Mater. Sci. Eng. 14 (2006) 515.
[62] F. Aguado, V.G. Baonza, Phys. Rev. B 73 (2006) 024111.
[63] S. Adachi, Properties of Group-IV, III–V and II–VI Semiconductors, Wiley, UK, 2005;
H.Y. Jun, C. Yan, W.Y. Ju, C.X. Rong, Chin. Phys. 16 (01) (2006) 0217.
[64] P. Hohenberg, W. Kohn, Phys. Rev. 136 (1964) 864.
[65] W. Kohn, L.J. Sham, Phys. Rev. 140A (1965) 1133.
[66] W.E. Pickett, Comput. Phys. Rep. 9 (1989) 117.
[67] J.P. Perdew, Y. Wang, Phys. Rev. B 45 (1992) 13244.
[68] J.P. Perdew, K. Burke, M. Emzerhof, Phys. Rev. Lett. 77 (1996) 3865.
[69] E. Engel, S.H. Vosko, Phys. Rev. B 47 (1993) 13164.
[70] P. Dufek, P. Blaha, K. Schwarz, Phys. Rev. B 50 (1994) 7279.
[71] C. Persson, R. Ahuja, B. Johansson, Phys. Rev. B 64 (2001) 033201.
[72] A. Mokhatari, H. Akbarzadeh, Physica B 324 (2002) 305.
[73] A. Mokhatari, H. Akbarzadeh, Physica B 337 (2003) 122.
[74] A. Mokhtari, H. Akbarzadeh, J. Phys.: Condens. Matter 16 (2004) 6063.
[75] R. Ahmed, H. Akbarzadeh, Fazal-e-Aleem, Physica B 370 (2005) 52.
[76] A. Zaoui, F. El Haj Hassan, J. Phys.: Condens. Matter 13 (2001) 253.
[77] F. El Haj Hassan, H. Akbarzadeh, Mater. Sci. Eng., B 121 (2005) 170.
[78] R. Ahmed, S.J. Hashemifar, H. Akbarzadeh, M. Ahmed, Fazal-e-Aleem, Comput. Mater. Sci. 39 (2007) 580;
B. Amrani, R. Ahmed, F. El Haj Hassan, Comput. Mater. Sci. 40 (2007) 66.
[79] A. Bouhemadou, R. Khenata, F. Zegrar, M. Sahnoun, H. Baltache, A.H. Reshak, Comput. Mater. Sci. 38 (2006) 263.
[80] G.K.H. Madsen, P. Blaha, K. Schwarz, E. Sjostedt, L. Nordstrom, Phys. Rev. B 64 (2001) 195134;
P. Blaha, K. Schwarz, G.K.H. Madsen, D. Kvasnicka, J. Luitz, WIEN2k, An Augmented Plane Wave + Local Orbitals Program for Calculating Crystal Properties, Karlheinz Schwarz, Techn. Universität Wien, Austria, 2001, ISBN 3-9501031-1-2;
K. Schwarz, P. Blaha, G.K.H. Madsen, Comp. Phys. Commun. 147 (2002) 71.
[81] K. Schwarz, P. Blaha, Quantum Mechanical Computations at the Atomic Scale for Material Sciences, WCCM V, July 7–12, 2002, Vienna, Austria.;
K. Schwarz, P. Blaha, Comput. Mater. Sci. 28 (2003) 259 ⟨http://www.wien2k.at⟩.
[82] R.W.G. Wyckoff, Crystal Structures, second ed., Krieger, Malabar, 1986;
O. Madelung, Semiconductors: Data Handbook, Springer, Berlin, 2004;
⟨http://cst-www.nrl.navy.mil/lattice/⟩.
[83] P.E. Blochl, O. Jepsen, O.K. Andersen, Phys. Rev. B 49 (1994) 16223.
[84] F.D. Murnaghan, Proc. Natl. Acad. Sci. USA 30 (1944) 244.